(19) Lukáč, I.; Hrdlovič, P. *Eur. Polym. J.* **1979**, *15*, 533.
(20) See ref 17 for a figure showing the transient spectrum.
(21) Wagner, P. J. *Acc. Chem. Res.* **1971**, *4*, 168.
(22) The lifetime of the triplet state of poly(phenyl vinyl ketone) has been estimated as 55 ns in benzene at room temperature.[14]
(23) Wagner, P. J.; Kemppainen, A. E.; Schott, H. N. *J. Am. Chem. Soc.* **1970**, *92*, 5280. *Ibid.* **1973**, *95*, 5604. *Ibid.* **1973**, *95*, 5604.
(24) Small, R. D., Jr.; Scaiano, J. C. *Chem. Phys. Lett.* **1977**, *50*, 431.
(25) For example, 1,3-pentadiene quenches *p*-methoxyacetophenone triplets in benzene (293 K) with $k_q = 6.4 \times 10^9$ $M^{-1}$ $s^{-1}$.
(26) Murov, S. L. "Handbook of Photochemistry"; Marcel Dekker: New York, 1973; p 89.
(27) E.g.: O'Connell, E. J., Jr. *J. Am. Chem. Soc.* **1968**, *90*, 6550. Klöpffer, W. *J. Polym. Sci., Polym. Symp.* **1976**, *No. 57*, 205.
(28) Scaiano, J. C. *J. Photochem.* **1973/1974**, *2*, 81.
(29) Das, P. K.; Encinas, M. V.; Steenken, S.; Scaiano, J. C. *J. Am. Chem. Soc.*, **1981**, *103*, 4162.
(30) Wagner, P. J.; Nakahira, T. *J. Am. Chem. Soc.* **1973**, *95*, 8474.
(31) Encinas, M. V.; Funabashi, K.; Scaiano, J. C. *Macromolecules* **1979**, *12*, 1167.
(32) Since in order to generate a quencher at the end of the chain it is necessary to fragment the macromolecule, the molecules responsible for the fast decay are expected to be shorter than the average. Dividing by 2 is a course approximation that neglects the fact that these short molecules are also counted in the average molecular weight.
(33) Montroll, E. W. *J. Math. Phys.* **1969**, *10*, 753.
(34) Montroll, E. W. *J. Phys. Soc. Jpn., Suppl.* **1969**, *26*, 6.
(35) Close approach is a condition for triplet energy transfer that can only take place by the exchange mechanism.[36,37]
(36) Terenin, A.; Ermolaev, V. *Trans. Faraday Soc.* **1956**, *52*, 1042.
(37) Förster, Th. *Discuss. Faraday Soc.* **1959**, *27*, 7.
(38) Since donor and acceptor are identical, either one could end up with the energy in the limiting case.
(39) Das, P. K.; Encinas, M. V.; Scaiano, J. C. *J. Photochem.* **1980**, *12*, 357.
(40) Das, P. K.; Scaiano, J. C. *Macromolecules* **1981**, *14*, 693.
(41) We have observed that small quenchers (e.g., 1,3-octadiene) quench faster the triplet states of polymers where no migration takes place. For example, quenching of a copolymer of PMA and methyl methacrylate is faster than of PPMA. The effect is quite general.[42]
(42) Lissi, E. A.; Scaiano, J. C., to be published.
(43) Loops of that size are less likely than smaller ones, due to the dependence of the cyclization probability with the size of the ring. See: Winnik, M. A. *Chem. Rev.*, in press.
(44) Some loop transfers between benzoyl and naphthalene moieties probably take place in MPN polymers;[40] however, exothermic transfers of that type are about 10 times more probable than isoenergetic triplet energy transfer of the type discussed in this section.[45]
(45) Encinas, M. V.; Scaiano, J. C. *Chem. Phys. Lett.* **1979**, *63*, 305.
(46) Freedman, H. H.; Mason, J. P.; Medalia, A. I. *J. Org. Chem.* **1958**, *23*, 76.
(47) Scaiano, J. C. *J. Am. Chem. Soc.* **1980**, *102*, 7747.

# Quasi-Elastic Light Scattering Studies of Semidilute Xanthan Solutions

**J. G. Southwick,* A. M. Jamieson, and J. Blackwell**

*Department of Macromolecular Science, Case Western Reserve University, Cleveland, Ohio 44106.* *Received May 13, 1980*

ABSTRACT: Quasi-elastic light scattering has been used to investigate the properties of xanthan gum in aqueous solution over a wide range of concentrations at low ionic strength. With increasing concentration, a transition is seen at a concentration $c^* \simeq 0.02\%$ as has been reported previously, which corresponds approximately to the onset of molecular overlap. We have now observed a second transition at a higher concentration, $c_2 \simeq 0.07\%$, where, in addition to a general reduction in the relaxation times, the single (polydisperse) relaxation mode observed below $c_2$ is replaced by bimodal behavior above the transition. Flow birefringence experiments show an intensity transition at $c_2$, corresponding to a sudden increase in anisotropy, indicative of intermolecular ordering at higher concentration. A possible interpretation of the bimodal behavior is that the $c_2$ transition is due to the development of more permanent intermolecular associations in xanthan solutions, which ultimately result in junction zones stabilizing a three-dimensional network. Of the two relaxation modes detected above $c_2$, the slow mode can be assigned to motions of the junction zones. Alternatively, the bimodal behavior is qualitatively similar to that predicted by Doi and Edwards for congested solutions of totally rigid rod macromolecules. In particular, the fast mode is concentration independent, while the slow mode is inversely proportional to concentration. However, the data show significant differences from those expected for fully extended chains and may be compatible with a broken-rod conformation for xanthan in solution.

## Introduction

The extracellular polysaccharide xanthan produced by the bacterium *Xanthomonas campestris* forms high-viscosity solutions when dissolved in water. This useful property has led to the commercial applications of this polysaccharide as xanthan gum. The chemical structure of xanthan[1,2] is a chain of (1→4)β-D-glucose residues with a trisaccharide substituent on alternate glucose residues. The side chain is β-D-mannopyranosyl-(1→4)-α-D-glucuropyranosyl-(1→2)β-D-mannopyranoside 6-*O*-acetate. In addition, the terminal D-mannose residue of the side chain may have a pyruvic acid residue linked to the 4 and 6 positions. The degree of pyruvate substitution typically varies from 0.31 to 0.56[3] and has been shown to be a function of the particular bacterial strain and fermentation conditions.[4,5] This distribution of the pyruvate groups on the xanthan chain has not been determined.

The rheological properties of xanthan solutions have been studied at different concentrations over a wide range of shear rates.[6] At low concentrations of xanthan, and for very low shear rates, Newtonian viscosity behavior was observed; in contrast, solutions of higher concentrations showed an apparent yield stress. Furthermore, it has been reported[7] that aqueous xanthan solutions at low ionic strength are birefringent at concentrations above 0.25%; in the presence of salt birefringence is seen for xanthan

*Address correspondence to J.G.S. at Shell Development Co., Houston, Texas 77001.

0024-9297/81/2214-1728$01.25/0 

concentrations greater than 0.5%. These observations suggest that intermolecular structures are formed in xanthan solutions at sufficiently high concentrations. In this paper we have used dynamic light scattering to study the molecular hydrodynamics of xanthan solutions over a range of concentration. Light scattering is a nonperturbing technique and therefore can be used to detect fragile intermolecular structures in solution; that is, the experiments are done in the absence of applied shear stress.

Our data are relevant to some recent theoretical studies[8-10] which use scaling theory to model the dynamical behavior of entangled flexible macromolecules in (semidilute) solutions. Polymer solutions at concentrations above the critical concentration for chain entanglements ($c^*$) have been modeled in terms of a temporary network, in which the dynamic characteristics are determined by the relaxation time of the entanglement points ($T_R$). It is argued that a dynamic light scattering experiment that detects concentration fluctuations having shorter relaxation times than $T_R$ will measure the diffusion of chain *segments* between these entanglement points and therefore will be insensitive to the center-of-mass diffusion of the entire molecule. For flexible chains in good solvents, scaling theory[8-10] predicts that above $c^*$ the length of chain segments between entanglement points ($\xi$) will decrease with increasing concentration ($c$):

$$\xi \propto c^{-0.75}$$

The cooperative diffusion coefficient of the chain segments, $D_c$, was also shown to be related to $\xi$ by a Stokes–Einstein equation, which leads to the prediction that

$$D_c \propto c^{0.75}$$

However, xanthan appears to have an ordered conformation in solution and also is a polyelectrolyte, for which we anticipate that scaling theories for flexible, uncharged chains will have limited validity. For semiflexible polymers, a mean field treatment predicts that $D_c \propto c^{0.5}$ at semidilute concentrations;[11] we have previously reported $D_c \propto c^{0.147}$ for xanthan.[12] Doi and Edwards[13,14] have developed a theoretical model for the behavior of rigid rod macromolecules in the concentration range $1/L^3 < c < 1/dL^2$ (where $L$ and $d$ are the length and diameter of the rods). The correlation function is nonexponential but rather resembles that for a bimodal exponential relaxation. The initial slope of a plot of ln $C(\tau)$ against $\tau$ is

$$\Gamma_1 = (1/3)D^0_{t\|}K^2$$

where $D^0_{t\|}$ is the limiting translational diffusion coefficient for motion parallel to the long axis. At longer times the correlation function decays exponentially with the characteristic time constant

$$\Gamma_2 = (K^2D_rD^0_{t\|})^{1/2}$$

where $D_r$ is the rotational diffusion coefficient of the rods. $\Gamma_2$ is dependent on the concentration, since it is predicted[15] that

$$D_r = D^0_r(cL^3)^{-2}$$

Thus $\Gamma_1$ is independent of concentration but $\Gamma_2$ is proportional to $1/c$.

In this paper we report a more detailed study of entangled solutions of xanthan, in which the data are discussed in terms of the above theoretical considerations. We observe a transition in the light scattering data at the overlap concentration ($c^*$) as well as a previously unreported cooperative transition at a higher concentration.

## Experimental Section

**Preparation of Solutions.** Samples of xanthan were obtained from the Kelco Co. (Kelzan) and purified by the method described by Holzwarth.[16] In a previous paper[17] we have determined for this sample that the molecular weight of an individual xanthan chain is $M = 2.16 \times 10^6$ and that these units self-associate with time to form larger structures. An aqueous solution of approximately 0.45% xanthan was prepared by addition of distilled water which had previously been filtered through 0.1-$\mu$m Millipore filters. This solution was then dialyzed for 4 days against distilled water. Sodium azide (0.02%) was added to the stock solution to retard bacterial growth, and aliquots of this solution were diluted with 0.02% aqueous sodium azide (0.1-$\mu$m filtered) to the final concentrations. Immediately prior to data collection the specimen solutions were filtered through 0.22-$\mu$m Millipore filters and centrifuged at $\sim$4500$g$. This allowed us to measure the diffusion properties of unaggregated xanthan and precluded the time-dependent effects which might complicate the interpretation. The final filtration is necessary to be certain that all bacterial cells are removed. We have checked our samples by electron microscopy and are confident that we report data for cell-free solutions. Filtration of dilute xanthan solutions through 0.22-$\mu$m Millipore filters resulted in a negligible loss in concentration of the polysaccharide, but such a filtration for the more concentrated solutions ($c > 0.1\%$) resulted in substantial losses. Thus, the final concentrations of the solutions were determined by evaporating the solution to dryness and weighing the residual film.

**Quasi-Elastic Light Scattering.** Laser light scattering experiments were performed on a digital photon correlation spectrometer. Radiation at 6328 Å from a He–Ne laser is focused into the solution; the scattered photons are detected by an ITT FW 130 phototube with a Pacific Photometrics discriminator/amplifier system, and the full correlation function is computed by a Honeywell Saicor SA-42 correlation and probability analyzer modified to permit digital photon correlation analysis. The sample cell was a 3-mL cylindrical Pyrex tube; this was immersed in a bath of decahydronaphthalene, which nearly matches the refractive index of glass, in order to reduce stray elastically scattered light. All correlation functions were determined by detecting the homodyne component of the scattered light.

**Flow Birefringence.** Solutions were circulated at a constant rate of shear through a capillary tube which was positioned between the polarizers of a Zeiss optical microscope. A Cole-Parmer Masterflex peristaltic pump was used in conjunction with a Cole-Parmer flow integrator in order to circulate the xanthan solutions at a constant rate. The intensity of the light transmitted through the crossed polarizers due to optical birefringence was measured with a Brinkmann photocell and a Simpson DC microammeter. Transmitted intensities were recorded for 0.03–0.18% xanthan solutions, and these data were corrected for intrinsic effects by subtraction of the intensity recorded using distilled water. The shear rate for this experiment was 2830 $s^{-1}$.

**Photon Correlation Analysis.** Since xanthan solutions typically exhibit nonexponential correlation functions, the (digital) data were analyzed by using a moment analysis procedure described by Brown et al.,[18] in which a polynomial function is fitted to points in the plot ln $C(\tau)$ against time:

$$\ln |C(\tau)| = -\bar{\Gamma}\tau + \frac{1}{2!}\frac{\mu_2}{\bar{\Gamma}^2}(\bar{\Gamma}\tau)^2 - \ldots$$

where $C(\tau)$ is the time correlation function. The initial slope of the plot ($\bar{\Gamma}$) is an averaged time constant related to the $z$-averaged translational diffusion coefficient

$$D_z = \bar{\Gamma}/K_2$$

where $K$ is the scattering wavevector. The nonexponentiality of the correlation function is characterized by the parameter $\mu_2/\bar{\Gamma}^2$, which is related to the degree of polydispersity in the sample. The experimental data points were also weighted as suggested by Pusey et al.[19]

The above treatment in inappropriate for systems exhibiting bimodal relaxation behavior, as is observed for xanthan solutions at higher concentrations, and for these the following procedure was applied. Correlation functions were obtained from a particular solution at many different correlation time increments ($\Delta\tau$). These

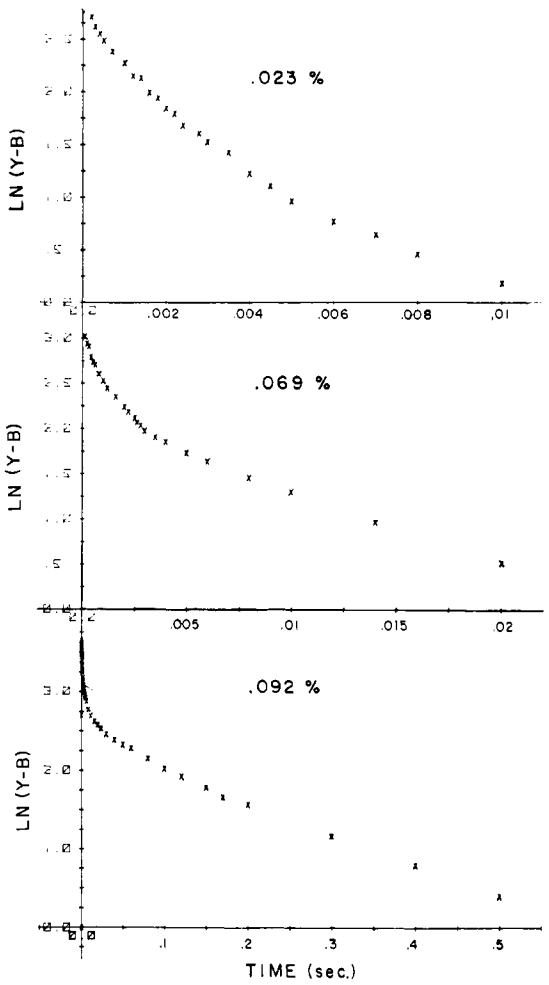


**Figure 1.** Plots of the logarithm of the correlation function vs. time for aqueous xanthan solutions at 0.023%, 0.069%, and 0.092% concentrations at low ionic strength (0.02% $NaN_3$). Data were collected at $\Theta = 40$ °C and 17 °C. $Y - B$ is the experimental measurement minus the background; $\ln (Y - B) = 2 \ln C(\tau)$.

correlation functions were then averaged by employing a linear least-squares fit of the experimental data points at the same sample time ($\tau$). In this manner the complete correlation function can be displayed with high resolution at short sample times. Correlation functions were matched nearly perfectly; the correlation coefficient was at least 0.99 in each case.

The bimodal behavior has been analyzed by using the following equation:

$$C(\tau) = A_1 \exp(-\Gamma_1 \tau) + A_2 \exp(-\Gamma_2 \tau) = (Y - B)^{1/2}$$

$Y$ is the experimental measurement of the intensity correlation function and $B$ is the background. $A_1$ and $A_2$ are the amplitudes and $\Gamma_1$ and $\Gamma_2$ are the time constants for the slow and fast modes, respectively. $A_1$ and $\Gamma_1$ are determined from the data at long times, for which there is essentially no contribution from the fast mode. The contribution of the slow mode can then be subtracted from the correlation function at shorter times, leading to determination of $A_2$ and $\Gamma_2$ for the fast mode.

## Results

The correlation functions for xanthan in deionized water were plotted as $\ln (Y - B)$ against time; three such plots for xanthan solutions of 0.023%, 0.069%, and 0.092% are shown in Figure 1. The plot for the 0.023% xanthan solution shows a significant degree of curvature, which is probably due to the distribution of molecular weights. The data for solutions of 0.004% and 0.0115% were similar to the 0.023% plot in that they were indicative of a single, polydisperse relaxation mode. However, the curves for the

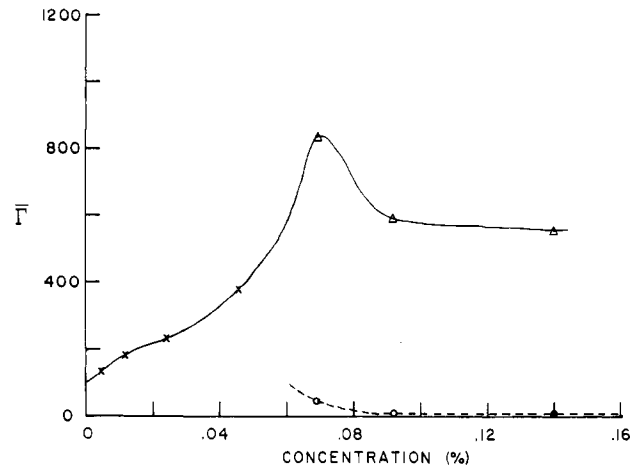


**Figure 2.** Time constants plotted against concentration for low ionic strength (0.02% $NaN_3$) aqueous xanthan solutions. (×) values determined from single-mode correlation functions. For bimodal correlation functions the fast mode is represented as Δ, and the slow mode as O.

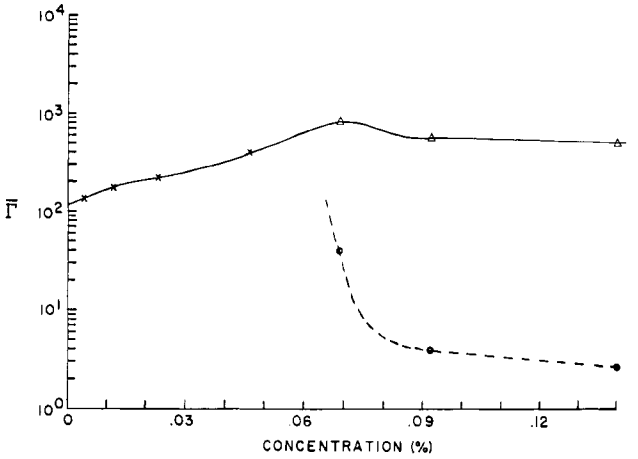


**Figure 3.** Time constants plotted against concentration on a semilog scale for low ionic strength (0.02% $NaN_3$) aqueous xanthan solutions. The single-mode and bimodal data are represented as in Figure 2.

0.069% and 0.092% solutions show a discontinuous change in slope and appear to become linear at longer correlation times ($\tau > 0.005$ s). At shorter correlation times, the plots show a degree of curvature similar to that observed in the 0.023% plot. The data obtained for a 0.14% xanthan solution are qualitatively similar to the 0.092% plot.

The first moments ($\bar{\Gamma}$) determined from the correlation functions are plotted against concentration in Figure 2. It is seen from this plot that $\bar{\Gamma}$ increases with concentration up to approximately 0.0125%, passes through an inflection, and continues to increase to $c \simeq 0.07\%$. At higher concentrations, the correlation functions become bimodal, indicating that fast and slow relaxation processes coexist in solution. $\Gamma_1$ and $\Gamma_2$ are shown in Figure 2 at concentrations above 0.07%; their dependence on concentration is seen more easily in Figure 3, where $\log \bar{\Gamma}$ is plotted against concentration. The time constant for the fast mode, $\Gamma_2$, decreases sharply and then continues to decrease more slowly, with $\Gamma_1$ approximately proportional to $1/c$.

Figure 4 shows the concentration dependence of the birefringence of xanthan solutions; the difference between the intensities of light transmitted through crossed polarizers for mobile and stationary xanthan solutions is plotted against concentration. It is seen that there is a change in the slope of the curve at a concentration of

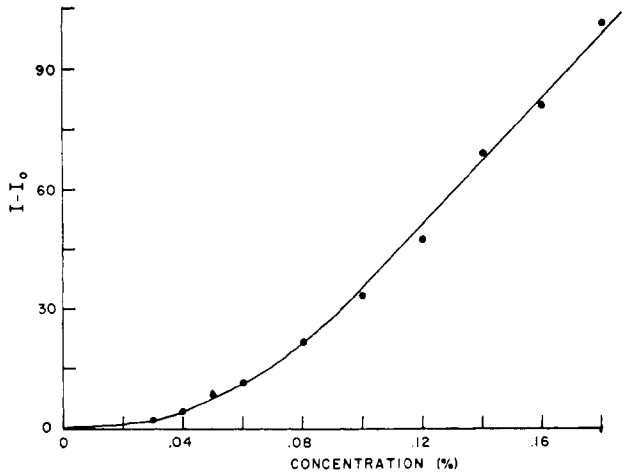


**Figure 4.** Flow birefringence of xanthan solutions plotted as a function of concentration. The birefringence is calculated as the difference between the intensities of light transmitted through crossed polarizers for a xanthan solution and deionized water. The measurements were made at a shear rate of 2830 $s^{-1}$.

~0.06%, above which the change in the transmitted intensity with concentration is nearly linear.

## Discussion

The data show that for solutions of xanthan in deionized water a hydrodynamic transition occurs at a concentration $c > c^*$. This transition is apparent at a xanthan concentration of ~0.07%, designated $c_2$. As mentioned above, abrupt changes in the hydrodynamic properties are expected at the critical concentration $c^*$ for the overlap of molecular domains; however, the observed transition at $c_2$ corresponds to a higher concentration effect. $c^*$ can be estimated from the following equation:

$$c^* \simeq 0.75\bar{M}/(4/3)\pi(R_h)^3N_A$$

based on $\bar{M} = 2.16 \times 10^6$ and $R_h = 1400$ Å (calculated from $D^0_t = 1.40 \times 10^{-8}$) which gives $c^* \simeq 0.023\%$. This calculation assumes a spherical particle, and the anisotropy of the xanthan chain will result in an even lower value of $c^*$, which is much lower than $c_2$.

The $c_2$ transition corresponds to two major effects in the quasi-elastic light scattering data: first, a transition from a single (polydisperse) relaxation mode to bimodal relaxation behavior principally due to the appearance of an additional slow relaxation mechanism, and second, a general slowing down of the relaxation times. One possible explanation of the $c_2$ transition is that it is due to a transition in xanthan solutions in which (nonpermanent) junction zones are formed at $c_2$ through intermolecular alignment of the *stiff* xanthan chain segments, and it is the diffusion of these junction zones through the solution that is the source of the slow relaxation process. The fast relaxation process would correspond to the diffusion of nonaligned chain segments, i.e., sections of the chains between junction zones.

This interpretation is consistent with the birefringence data presented in Figure 4. The modest flow birefringent effect detected for concentrations $c < c_2$ is due to the alignment of individual molecules in the flow field. However, for concentrations $c > c_2$ an enhancement of the birefringence indicates an increased tendency to form ordered structures at higher concentrations.

The formation of junction zones at $c_2$ can be interpreted in terms of an entropy-driven phase separation phenomenon. Such phase separations are predicted[20] theoretically for rigid rod particles and have been observed for solutions of tobacco mosaic virus (TMV).[21-23] Above a critical concentration, TMV particles separate into an efficiently packed high-concentration ordered phase and a dilute disordered phase. A similar process is envisaged for xanthan except that the long length and limited flexibility of the chains, and the associated entangled structure, prevent complete phase separation. Thus a given chain will connect both the polymer-rich phase (the junction zones) and the polymer-poor phase (chains between junction zones), and a localized fringed micelle structure is formed.

Table I
Comparison of Experimental and Theoretical Doi-Edwards Parameters for Xanthan Models[a]

| concentration, % | $D^0_{t\|\|}$, $cm^2/s$ | $D_r$, $s^{-1}$ (obsd) | $D_r$, $s^{-1}$ (calcd)[b] |
|---|---|---|---|
| 0.069 | $3.03 \times 10^{-7}$ | $6.70 \times 10^{-1}$ | $1.6 \times 10^{-5}$ |
| 0.092 | $2.18 \times 10^{-7}$ | $8.25 \times 10^{-3}$ | $1.0 \times 10^{-5}$ |
| 0.14 | $2 \times 10^{-7}$ | $4.11 \times 10^{-3}$ | $0.4 \times 10^{-5}$ |

[a] Calculated values of $D^0_{t\|\|}$ and $D_r$ from correlation functions for solutions at $c \geq c_2$. [b] Rod with dimensions $L = 15\,000$ Å, $d = 20$ Å, and $M = 2 \times 10^6$; $c^* = 1/L^3 = 10^{-4}\%$.

Whitcomb and Macosko[6] have obtained evidence which suggests a yield stress for xanthan solutions at a concentration of 1%. It is possible that the transition in our light scattering data at ~0.07% is the earliest indication of an intermolecular ordering in xanthan and that with increasing concentration the size and number of these ordered regions increase to a point where they are detected in a rheological experiment. However, the effect reported by Whitcomb and Macosko is manifested in a plot of shear stress against shear rate as a very narrow horizontal region at the lowest available shear rate. Indeed, it has been reported[24] that the time-dependent shear compliance of xanthan solutions in this concentration regime indicates there is no true yield stress. Thus the junction zones, if they exist, are time-dependent structures, easily destroyed by shear forces.

As an alternative interpretation, the bimodal correlation functions are qualitatively similar to the behavior predicted by Doi and Edwards for solutions of totally rigid rods. The slow relaxation mode is due to rotation that is severely restricted by the cagelike structure of neighboring rods, while the fast mode corresponds to the translational motion of the rod along its long axis. Neutron diffraction data[7] for birefringent solutions suggest a cylindrical particle, 12 000 Å in length and 60 Å in width. Hydrodynamic data also favor a rod-shaped particle, in this case with dimensions 15 000 × 20 Å. However, Whitcomb and Macosko[6] indicate that the latter data do not precisely fit the predictions for a rigid rod, and these authors suggest a broken-rod model. Based on the X-ray fiber repeat, a fully extended xanthan chain with a molecular weight $2 \times 10^6$ would have a length of approximately 20 000 Å and a width of 20 Å; this molecule would be expected to buckle in solution due to the high bending moments. It should be noted that quiescent birefringence is difficult to achieve in xanthan solutions and requires equilibration for extended periods in the cold.[7] Also, the flow birefringence transition indicated in Figure 4 could reflect shear-induced transition to a liquid crystal phase.[25] Each of these observations suggest a degree of flexibility in the xanthan molecule.

Table I presents the values of $D^0_{t\|}$ and $D_r$ calculated from the correlation functions for solutions at concentra-

tion $c > c_2$. Above $c_2 = 0.07\%$ the fast mode is approximately constant while the slow mode is approximately proportional to $1/c$, as predicted by Doi and Edwards. Table I also shows calculated values of $D_r$ for the rod structure 15000 × 20 Å. The calculated values are several orders of magnitude smaller than experiment. However, the Doi-Edwards theory does not take account of electrostatic repulsions, and this could account partially for the discrepancies.

Based on the above discussion, it is not possible to make a clear choice as to the origin of the hydrodynamic transition observed in xanthan solutions at $c \sim c_2$. It seems likely that the charged xanthan molecule has a semirigid structure, and therefore a quantitative application of the Doi-Edwards theory is not justified. It is pertinent to note, however, that Lee et al.[26] have argued that the hydrodynamics of congested solutions of semiflexible chains can be treated by a dynamical equation equivalent to that of Doi and Edwards, again leading to the prediction of bimodal decays in the dynamic structure factor. On the other hand, a broken-rod structure of xanthan would lead to intermolecular contacts along localized sequences and thus facilitate the formation of junction zones.

**Note Added in Proof.** Subsequent experiments, in which the diffusion of latex microspheres in semidilute xanthan solutions was studied, are consistent with the existence of a motionally restricted isotropic network of long thin fibers. This suggests that the Doi-Edwards theory should be applicable in the range $1.0 < c < 3.5$ g/L (Jamieson, A. M.; Southwick, J. G.; Blackwell, J. *J. Polym. Sci., Polym. Phys. Ed.*, submitted). The quantitative discrepancy between theory and experiment noted above implies that the critical entanglement length for onset of constrained diffusion is substantially smaller than the whole rod length. This effect has been observed for other rodlike macromolecules (Jain, S.; Cohen, C. *Macromolecules* **1981**, *14*, 759).

**Acknowledgment.** This research was supported by NSF Grant No. PCM-18631.

## References and Notes

(1) Jansson, P. E.; Keene, L.; Lindberg, B. *Carbohydr. Res.* **1975**, *45*, 275.
(2) Melton, L. D.; Mindt, L.; Rees, D. A.; Sanderson, G. R. *Carbohydr. Res.* **1976**, *46*, 245.
(3) Sandford, P. A.; Watson, P. R.; Knutson, C. A. *Carbohydr. Res.* **1978**, *63*, 253.
(4) Cadmus, M. C.; Rogovin, S. P.; Burton, K. A.; Pittsley, J. E.; Knutson, C. A.; Jeannes, A. *Can. J. Microbiol.* **1976**, *22*, 942.
(5) Cadmus, M. C.; Knutson, C. A.; Lagoda, A. A.; Pittsley, J. E.; Burton, K. A. *Biotechnol. Bioeng.* **1978**, *20*, 1003.
(6) Whitcomb, P. J.; Macosko, C. W. *J. Rheol.* **1978**, *22*, 493.
(7) Rinaudo, M.; Milas, M.; Duplessix, R. *IUPAC 26th Symp. Macromol., Makro Mainz* **1979**, 800.
(8) Daoud, M.; Cotton, J. P.; Farnoux, B.; Jannink, G.; Sarma, G.; Benoit, H.; Duplessix, R.; Picot, C.; de Gennes, P. G. *Macromolecules* **1975**, *8*, 804.
(9) de Gennes, P. G. *Macromolecules* **1976**, *9*, 587.
(10) de Gennes, P. G. *Macromolecules* **1976**, *9*, 594.
(11) Schaefer, D. W.; Joanny, J. F.; Pincus, P. *Macromolecules* **1980**, *13*, 1280.
(12) Southwick, J. G.; McDonnell, M. E.; Jamieson, A. M.; Blackwell, J. *Macromolecules* **1979**, *12*, 305.
(13) Doi, M.; Edwards, S. F. *J. Chem. Soc., Faraday Trans. 2* **1978**, *74*, 560.
(14) Doi, M.; Edwards, S. F. *J. Chem. Soc., Faraday Trans. 2* **1978**, *74*, 918.
(15) Doi, M. *J. Phys. (Paris)* **1975**, *36*, 607.
(16) Holzwarth, G. *Biochemistry* **1976**, *15*, 4333.
(17) Southwick, J. G.; Jamieson, A. M.; Blackwell, J., submitted to *Carbohydr. Res.*
(18) Brown, J. C.; Pusey, P. N.; Dietz, R. *J. Chem. Phys.* **1975**, *62*, 1136.
(19) Pusey, P. N.; Koppel, D. E.; Schaefer, D. W.; Camerini-Otero, R. D.; Koenig, S. H. *Biochemistry* **1974**, *13*, 952.
(20) Flory, P. J. *Proc. R. Soc. London, Ser. A* **1956**, *234*, 73.
(21) Bawden, F. C.; Pirie, N. W. *Proc. R. Soc. London, Ser. B* **1937**, *123*, 274.
(22) Bernal, J. D.; Fankucken, I. *J. Gen. Physiol.* **1941**, *25*, 111.
(23) Oster, G. *J. Gen. Physiol.* **1950**, *33*, 445.
(24) Mitchell, J. R. In "Polysaccharides in Foods"; Blanshard, J. M. V., Mitchell, J. R., Eds.; Butterworth: London, 1979.
(25) Valenti, B.; Ciferri, A. *J. Polym. Sci., Polym. Lett. Ed.* **1978**, *16*, 657.
(26) Lee, W. I.; Schmitz, K.; Lin, S. C.; Schurr, J. M. *Biopolymers* **1977**, *16*, 583.

# Reptation in Entangled Polymer Solutions by Forced Rayleigh Light Scattering

**L. Léger,* H. Hervet, and F. Rondelez**

*Laboratoire de Physique de la Matière Condensée, Collège de France, 75231 Paris Cedex 05, France.* *Received March 5, 1981*

ABSTRACT: We have measured the self-diffusion coefficient of polystyrene chains in benzene solutions as a function of both concentration $C$ and molecular weight $M$, using a forced Rayleigh light scattering technique. In the semidilute regime where the chains overlap, we obtain $D_{self} \sim C^{-\alpha}M^{-\beta}$, with $\alpha = 1.7 \pm 0.1$ and $\beta = 2 \pm 0.1$, in good agreement with scaling and reptation predictions. Measurements on mixed systems, with labeled chains shorter than their neighbors, demonstrate for the first time the weakness of the tube renewal processes in semidilute polymer solutions.

## Introduction

Entangled polymer solutions have very unusual viscoelastic behavior. Much effort, both experimental and theoretical, has been devoted to unravel their dynamical properties; however, they are not yet completely elucidated. The difficulty is to correctly take into account the effect of chain disentanglements. The recent scaling approach[1,2] has made a significant contribution to the understanding of chain dynamics by pointing out that a large class of motions, the so-called collective motions, do not require chain disentanglements.[3] Then, when performing a dynamic experiment, one has to distinguish carefully between collective and individual chain motions, i.e., monomer motions respectively without or with relative displacements of the center of mass of the chains. Both contributions are usually important, but some experiments allow separation of them. Following ref 3, the collective motions of the chains can be described in terms of a cooperative diffusive mode, characterized by a diffusion coefficient $D_{coop} \sim \xi^{-1}$, where $\xi$ represents the average distance between entanglements. $\xi$ is independent of the polymerization index $N$, and its concentration dependence can

0024-9297/81/2214-1732$01.25/0 